Available online at www.sciencedirect.com

ScienceDirect

Procedia 00 (2018) 000–000

www.elsevier.com/locate/procedia

10th Conference on Photonic Technologies – LANE 2018

# Analytical prediction of laser mediated polymer melt and damage width

Colin Frank Dowding [a] *, Jonathan David Griffiths[a], Mark Swainson[b]

[a] *School of Engineering, University of Lincoln, Lincoln, Lincolnshire, LN6 7TS. UK*
[b] *National Centre of Food Manufacturing, University of Lincoln, Park Road, Holbeach, PE12 7PT. UK*
* Corresponding author. Tel.: +44-0152-2837-914. *E-mail address:* cdowding@lincoln.ac.uk

**Abstract**

Far-field (remote) laser net-shape scanning has revolutionary potential across numerous applications which involve localized heating of materials. It offers a very high degree of manufacturing flexibility in concert with process repeatability, traceability and low cycle energy usage when compared to traditional tooling-based solutions if the material response can be accurately predicted.

The functional mechanism of such processes is localized heating; in this work, an analytical model of the line width of phase change occurring between a 3mm thick virgin polypropylene, PP, sheet and a visually transparent 25µm thick PP film is presented.

Validation of the model is provided empirically by the scanned application of a $CO_2$ laser exhibiting a Gaussian beam profile onto reference materials at varying incident spot diameters, powers and traverse velocities.

This work is of value for process parameter prediction, as this analytically based method is computationally light, enabling its real-time implementation in manufacturing environments.



*Keywords:* “Net-shape”, “Polymer”, “Melt”, “Width”, “Prediction”.

## 1. Introduction

Far-field (remote) laser irradiation of materials presents opportunities for the rapid and flexible processing of complex net-shape features [1]. Laser processing of moderate-to-high transparency materials, particularly polymers, offers increased component complexity [2]. The thermodynamics of highly absorbent materials for the purposes of drilling, cutting, welding and other melt-based processes are highly developed [3]; however, a more complex scenario (e.g. polymers), where a keyhole is undesirable and the volumetric heat source provided by the laser beam is greatly reduced by the transparent nature of the material, is less successfully modelled.

The low melting and thermal degradation temperatures of polymers, coupled with their low thermal diffusivity, means that such materials are highly sensitive to process parameter modulation [4]. Many researchers have investigated the use of laser sources for the thermal bonding (*via* adhesive and welding methodologies) for the direct benefit of the packaging industry [5]. A subject of great concern for food packaging is that of volatile and/or toxic fumes resultant from excessive heating by any thermal source during sealing [6]. To date, the geometric properties of the beam have not been sufficiently considered to allow the accurate prediction of the real-time seal width resultant from operational parameters or to predict combustion of the polymer, leading to the generation of unwanted fumes.

To bond, first there must be melting; this model will be used to predict melt track widths. Such information could be used to infer bond width. A response surface approach [7] will be used to assess the validity of an analytically derived model which predicts the volumetric temperature rise of a Gaussian laser beam of a known incident power and spot diameter, traversing at a known incident velocity across a material with well understood optical and thermodynamic properties at the laser’s wavelength. The model developed is intended for computationally efficient process parameter prediction. This work will use unpigmented homopolymer polypropylene (PP), irradiated by a $CO_2$ laser as a reference scenario.

## 2. Model Development

### *2.1. Spatially Discretized Irradiant Exposure*

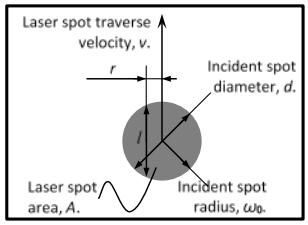


Fig. 1. Representation of a circular laser spot traversing a static surface.

A laser beam energy density presented to a region of material as an incident spot, with a power, $P_0$, traverses across a flat plane of material lying bi-normal to the beam, as shown in Fig. 1, can be considered as an irradiant exposure:

$$I_{SCAN} = \frac{E}{A} = \frac{P_0}{\pi.\omega_0^2}.\frac{l}{v}\ [\mathrm{J/m^2}]; \qquad (1)$$

multiplying by area and considering the light which isn't reflected yields an absolute energy exposure value:

$$Q = (1-R)I_{SCAN}.A\ [\mathrm{J}]. \qquad (2)$$

For a given strip (of discretized width, $\Delta r$, and radius dependent length, $l = 2l_\omega$) which lies parallel to the direction of incident spot traversal within a circular incident spot, the localized energy exposure can be considered:

$$Q = \frac{(1-R)P_0}{\pi.\omega_0^2}.\frac{l}{v}.\Delta r.l\ [\mathrm{J}]. \qquad (3)$$

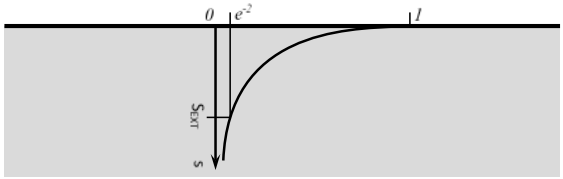


Fig. 2. Schematic of intensity propagation used in analytical model.

Integration of the Beer-Lambert law over a discrete inspection length at a known propagation depth allows the generation of a spatially dependent coupling coefficient following the relationship described schematically in Fig. 2:

$$Q_{\Delta s} = \frac{(1-R)P_0}{\pi.\omega_0^2}.\frac{l}{v}.\Delta r.l.\left[e^{-\alpha(s-\Delta s)} - e^{(-\alpha s)}\right]\ [\mathrm{J}]. \qquad (4)$$

The Gaussian intensity profile of the beam can be considered as a spatially dependent coefficient generated by integrating the radius dependent Gaussian intensity relationship (Eq. 5) with respect to $l_\omega$, as shown in Fig. 3:

$$\int_0^{l_\omega} I_r\,dl = \frac{2(1-R)P_0}{\pi.\omega_0^2}\left[\frac{1}{2}\sqrt{\frac{\pi}{2}}\omega_0 e^{\left(\frac{-2r^2}{\omega_0^2}\right)} erf\left(\frac{\sqrt{2}l}{\omega_0}\right)\right]_{l=0}^{l=l_\omega} \qquad (6)$$

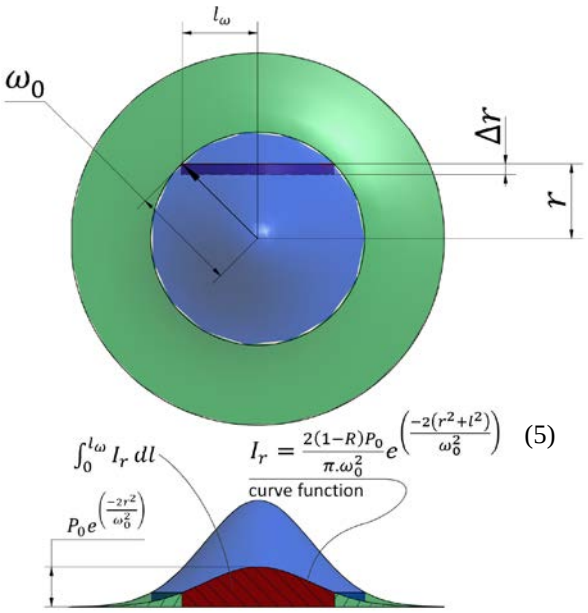


(5)

Fig. 3. Orientation dependent discretization of circular Gaussian distributions.

since erf(0) = 0 and from Pythagoras: $l_\omega = \sqrt{\omega_0^2 - r^2}$:

$$\int_0^{l_\omega} I_r\,dl = \frac{(1-R)P_0}{\pi.\omega_0^2}\left[\sqrt{\frac{\pi}{2}}\omega_0 e^{\left(\frac{-2r^2}{\omega_0^2}\right)} erf\left(\frac{\sqrt{2}.\sqrt{\omega_0^2-r^2}}{\omega_0}\right)\right]. \qquad (7)$$

To take the entire beam diameter into account, Eq. 7 must be doubled. This 'plane of energy' must then be multiplied by the discretized exposure strip to yield irradiant exposure. Once complete, the Irradiant Exposure of a strip running like a cord across a circular Gaussian beam at a known radius can be converted into an energy exposure prediction:

$$Q = \frac{4(1-R)P_0\left[\sqrt{\frac{\pi}{2}}\omega_0 e^{\left(\frac{-2r^2}{\omega_0^2}\right)} erf\left(\frac{\sqrt{2}.\sqrt{\omega_0^2-r^2}}{\omega_0}\right)\right]\Delta r\sqrt{\omega_0^2-r^2}\left[e^{-\alpha(s-\Delta s)} - e^{(-\alpha s)}\right]}{\pi.\omega_0^2.v}\ [\mathrm{J}]. \qquad (8)$$

### *2.2. Heat to Melt, $dT_M$*

The low thermal diffusivity of polymers (≈0.1x10$^6$ m$^2$.s$^{-1}$) [8] presents the opportunity to avoid consideration of thermal conduction and use a heat transfer relation to relate temperature rise in a material to energy exposure:

$$Q = (m \cdot C_P \cdot dT) + (m \cdot H_m); \qquad (9)$$

where $H_m$ is the latent heat of fusion, $C_P$ is the specific heat capacity, $\rho$ is the density of the material being heated and

$$m = \rho.\Delta s.\Delta r.2\sqrt{\omega_0^2 - r^2}. \qquad (10)$$

Substitution of this thermal energy relation into the energy exposure definition (Eq.8) and simplifying yields:

$$dT_M = \frac{2(1-R)P_0.\left[\sqrt{\frac{\pi}{2}}.e^{\left(\frac{-2r^2}{\omega_0^2}\right)}.erf\left(\frac{\sqrt{2}.\sqrt{\omega_0^2-r^2}}{\omega_0}\right)\right]\left[e^{-\alpha(s-\Delta s)} - e^{(-\alpha s)}\right]}{\pi.\omega_0.v.C_P.\rho.\Delta s}$$

$$-\left(\rho.\Delta s.\Delta r.2\sqrt{\omega_0^2 - r^2}\,H_m\right). \qquad (11)$$

### 2.3. Heat to Combust, dTC

Similarly, the energy requirement for combustion is:

$$Q = (m \cdot C_P \cdot dT) + \left(m \cdot (H_m + H_C)\right); \quad (12)$$

where $H_C$ is the heat of combustion. Substituting these relations into the energy exposure relation (Eq. 8) yields:

$$dT_C = \frac{2(1-R)P_0 \cdot \left[\sqrt{\frac{\pi}{2}} \cdot e^{\left(\frac{-2r^2}{\omega_0^2}\right)} \cdot erf\left(\frac{\sqrt{2} \cdot \sqrt{\omega_0^2 - r^2}}{\omega_0}\right)\right] \left[e^{-\alpha(s-\Delta s)} - e^{(-\alpha s)}\right]}{\pi \cdot \omega_0 \cdot v \cdot C_P \cdot \rho \cdot \Delta s}$$

$$- \left(\rho \cdot \Delta s \cdot \Delta r \cdot 2\sqrt{\omega_0^2 - r^2}\,(H_m + H_C)\right). \quad (13)$$

## 3. Empirical Validation

The equations described in Section 2 were used to compare the temperature rise within a thin layer of polymer at a known propagation depth with respect to incident laser power, spot size and traverse velocity, as well as the distance of the point of interest from the centre line of the track irradiated. This temperature rise was then compared to the material's known melting and thermal degradation temperatures.

Section 2 has been applied to predict the widths at which a boundary layer, which lies between the bottom of a 25µm thick PP film (PP301025, Goodfellow Ltd.) and the top of a 3mm thick PP sheet (PP303030, Goodfellow Ltd.), either melts or combusts. Table 1 lists the material properties; the absorption coefficient was measured empirically to be $\alpha$ = -7969m$^{-1}$.

Predicted melt and damage widths are compared directly to empirical analogues generated by use of a $CO_2$ laser as shown in Fig. 4 applied using the process parameters given in Table 2.

Table 1. Relevant material properties of Polypropylene.

| Property | Value | Unit | Reference |
|---|---|---|---|
| Density ($\rho$) | 900 | kg.m$^{-3}$ | Supplier |
| Specific Heat Capacity ($C_P$) | 1800 | J.K$^{-1}$.kg$^{-1}$ | |
| Melting Temperature ($T_m$) | 170 | °C | |
| Thermal Breakdown Temp ($T_D$) | 369 | °C | |
| Latent heat of fusion ($H_m$) | 88x10$^3$ | J.kg$^{-1}$ | [9] |
| Heat of Combustion ($H_c$) | 4266x10$^4$ | J.kg$^{-1}$ | [10] |
| Reflectivity ($R$) | 0.04 | | [11] |

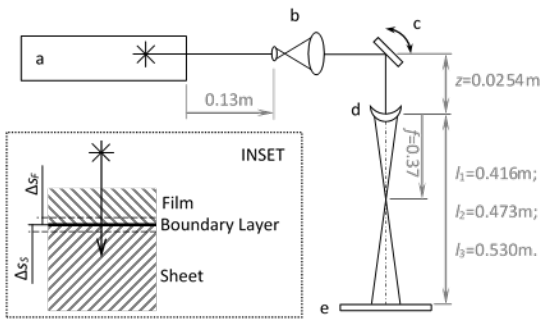


Fig. 4. Schematic laser processing arrangement incorporating: a) $CO_2$ laser (F201, Synrad); b) 3x beam expander; c) galvanometric beam deflection mirrors (Flyer FH, Synrad); d) F-Theta lens (Synrad); & e) irradiated sample. [INSET: schematic of beam propagation through sample arrangement].

Table 2. Experimental processing parameters incident at the sample.

| $P_0$ [W] | 40 | 60 | 80 | 100 | 120 | 140 | 160 | 180 |
|---|---|---|---|---|---|---|---|---|
| $V$ [m.s$^{-1}$] | 0.2 | 0.3 | 0.4 | 0.5 | 0.6 | 0.7 | 0.8 | |
| $\omega_0$ [mm] | 1.0 | 2.0 | 3.0 | | | | | |

Laser power was measured using a wavelength calibrated calorific thermopile (UP25N-250F-H12-D0, Gentec E-O) prior to the preparation of every sample; all incident traverse velocities are accurate at the surface of the sample, and the laser spot size is accurate (±0.1mm). $C_P$ was set at 1800 J.K$^{-1}$.kg$^{-1}$, this being the mean of the values quoted.

## 4. Results and Discussion

Melting widths at the boundary between the film and the sheet, as predicted using the model in Section 2, are plotted in Fig. 5 in concert with empirically gathered data points.

It is visually apparent that both the analytical prediction surface and the empirically gathered data points exhibit similar width magnitudes and trend shapes in all cases. The Chi squared, $\chi^2$, 'goodness of fit' factor is included with each plot in Fig. 5 to quantify the scale of variation between predicted and empirical results along with the sample population sizes, $n$. $\chi^2$ has been used to determine confidence intervals, see Table 3, concerning the null hypothesis that the prediction matches the empirical data. Such analysis demonstrates that, when predicting melting, a very high degree of correlation exists, but melting width under-prediction appears to develop with respect

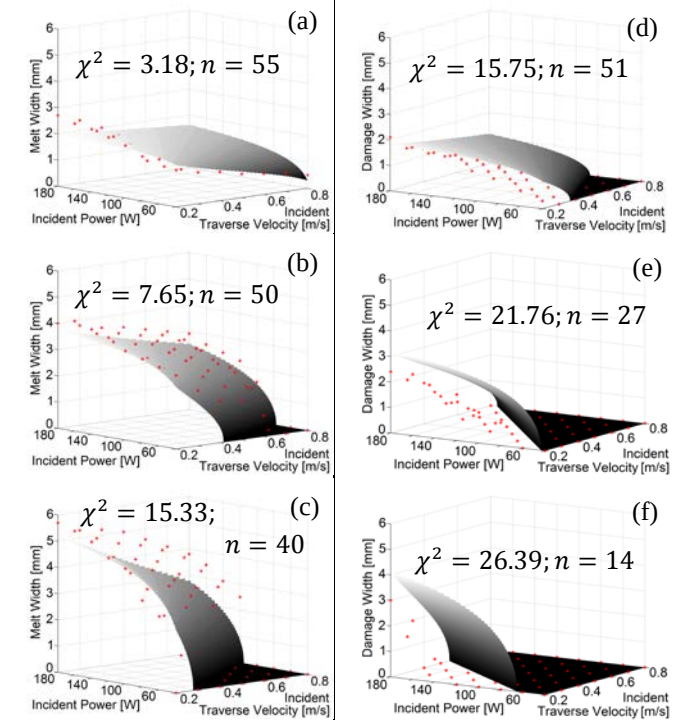


Fig. 5. Plots comparing prediction (surface) to empirical (*) data. Melting only: a) $\omega_0$=1mm; b) $\omega_0$=2mm; and c) $\omega_0$=3mm. Thermal damage only: d) $\omega_0$=1mm; e) $\omega_0$=2mm; and f) $\omega_0$=3mm.

Table 3. Quality indicators for prediction against empirical results in Fig 5.

| Fig 5. plot | a | b | c | d | e | f |
|---|---|---|---|---|---|---|
| $\chi^2$ Confidence [%] | >99.9 | >99.9 | >99.9 | >99.9 | >50 | >2.5 |
| *Mean error* [mm] | 0.14 | -0.34 | -0.26 | 0.45 | 0.54 | 0.53 |

to incident intensity. Thermal damage widths are universally over-predicted; exhibiting increased $\chi^2$ (and greatly reduced confidence) with respect to $I_{SCAN}$. Furthermore, the model delivers false damage predictions at larger irradiant exposures.

Melting width under-prediction is unlikely to be the result of an inaccurate $\alpha$, since absorption data for natural PP sourced from literature [3, 12, 13] (yielding values between 2000m$^{-1}$ - 3600m$^{-1}$) are under half that measured for this work; yet a larger $\alpha$ is required to correct the under-prediction. Melt width under-prediction is likely to indicate the inaccurate treatment of optical scattering within the material and the transverse electromagnetic (TEM) beam profile of the laser which is assumed to be ideally Gaussian in the model.

It is proposed that the fumes/flame developed (and witnessed) during combustion attenuated the beam *en-route* to the sample; reducing the interaction at the material surface yielding the gross over-prediction of damage widths in Fig. 5.

Fig. 6 combines the information conveyed in the melting and damage columns of Fig. 5 by plotting predicted melt widths until thermal damage set in. Any process parameter which lies under the volume of the surface in Fig. 6 will generate melting (potentially leading to a weld) without combustion.

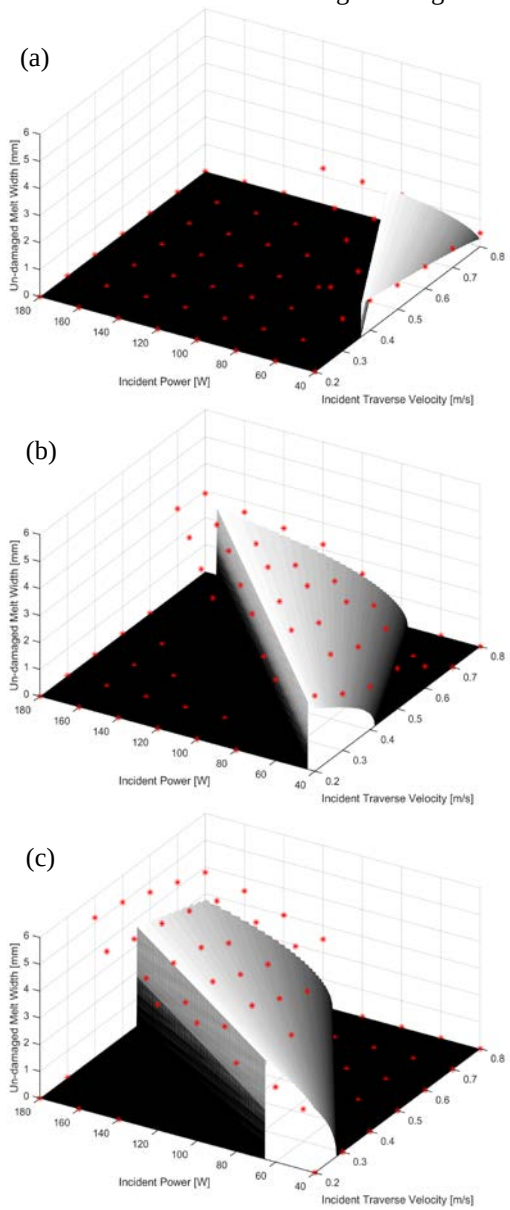


Fig. 6. Plots comparing predicted process parameters which yeild un-damaged melting to reality: a) $\omega_0$=1mm; b) $\omega_0$=2mm; and c) $\omega_0$=3mm.

Fig. 6 accentuates a major discrepancy between predicted and measured process parameter combinations which cause damage; the model universally predicts damage where none occurred. The model reports damage as soon as the material's thermal breakdown temperature is exceeded. In reality, the probability of damage builds from this temperature; it may be that physical damage did not occur to a detectable extent.

The introduction of a suplementary coating (with a lower melting temperature or increased $\alpha$), common practice in applications relevant to this work [14], would greatly broaden the operational windows under the surface volumes in Fig. 6.

## 5. Conclusions

An analytically derived, spatially discretized volumetric heating model is described which simulates the temperature rise of a region of a polymer irradiated by an incident Gaussian laser spot of a known size and traverse velocity to enable fume free welding. This model has been compared to empirical data gathered using a $CO_2$ laser and homopolymer polypropylene.

The model's melt width predictions exhibit a Chi squared confidence interval of at least 99.9% when compared to empirical data; melt and damage radius are proportional to power and inversely proportional to incident spot traverse velocity. Melt width under-prediction, although minor, develops with respect to irradiant exposure; this, in concert with false positive damage prediction indicates that the ideal Gaussian treatment of the transverse beam profile led to an under-prediction of the laser melting operational window. Combustion fumes witnessed also led to a gross reduction in damage width compared to that predicted.

This model is a viable real-time tool to facilitate automated laser process parameter prediction for polymer net-shape bonding with the provision of accurate materials data.

## References

[1] G. Reinhart, U. Munzert, W. Vogl (2008) *CIRP Annals* **57** (1) pp.37-40.
[2] J.P. Coelho, M.A. Abreu, M.C. Pires (2000) *Journal of Materials Processing Technology* **255** pp.808-815.
[3] W. W. Duley, R. E. Mueller (1992) *Polymer Engineering and Science* **32** (9) pp.582-585.
[4] C. F. Dowding, R. G. Dowding, F. Franceschini, J. D. Griffiths (2015) *Packaging Technology and Science*, **28** (7). pp.621-632.
[5] N. Brown, F. Shi, D. Kerr, M. R. Jackson, R. M. Parkin (2005) *Proceedings of the IMechE Part I:J Systems Control and Engineering* **219** pp.231-237.
[6] O. W. Lau, S. K. Wong. (2000) *Journal of Chromatography A*, **882** (1-2) pp.255-270
[7] B. Acherjee, D. Misra, D. Bose, K.Venkadeshwaran (2009) *Optics & Laser Technology* **41** pp.956.967.
[8] J. Blumm; A. Lindemann (2003/2007) *High Temperatures-High Pressures* **35/36** (6) p627.
[9] R. L. Blaine (2002) *Texas Instruments*, New Castle Google Scholar.
[10] R. N. Walters, S. M. Hackett, R. E. Lyon (2000) *Fire and Materials* **24** (5) pp.245-252.
[11] J. M. P. Coelho, M. A. Abreu, F. Carvalho Rodrigues (2004) *Polymer Testing* **23** (3) pp.307-312.
[12] P. T. Tsilingiris (2003) *Energy conversion and management*, **44** (18) pp.2839-2856.
[13] E. Bormashenko, R. Pogreb, A. Sheshnev, S. Sutovski, A. Shulzinger (2003) *Applied Surface Science* **220** (1-4) pp.125-135.
[14] N. M. Woosman (2005) *Proceedings of the ImechE Part D: Journal of Automobile Engineering* **219** (9) pp.1069-107